

Realizing any central projection with a mirror pair

R. Andrew Hicks, Marc Millstone, and Kostas Daniilidiis

We show that, for any rotationally symmetric projection with a single virtual viewpoint, it is possible to design a two-mirror rotationally symmetric system that realizes the projection exactly. These mirror pairs are derived from two coupled differential equations. We give examples in which the projections from the sphere at infinity are stereographic, perspective, and equiresolution. © 2006 Optical Society of America
OCIS codes: 080.2720, 080.2740.

1. Introduction

The term catoptric describes imaging systems that employ only mirrors. Catadioptrics employ a combination of mirrors and lenses. Traditionally, these terms have been associated with narrow field imaging, such as telescopes or lens designs such as the Schmidt and Maksukov–Cassegrain.¹ Nevertheless, by using a curved mirror in combination with a conventional camera and lens it is possible to create wide-angle or panoramic images. The use of curved mirrors for panoramic imaging dates back at least to the 1909 patent of Kleinschmidt, which combined a camera or lens with a conical mirror.² Since then, a multitude of panoramic catadioptric imaging devices have been designed.³

Increasing the field of view while keeping aberrations under control has always been a challenge for optical designers. The introduction of a curved mirror into an imaging system is an elegant solution to this problem, and in computer vision and robotics these devices have become known as catadioptric sensors. The recent interest in these sensors is largely because it is easy and inexpensive to build a wide-field of view or panoramic device with a rotationally symmetric con-

vex mirror. While the images may be highly distorted, they are amenable to rapid processing in software that transforms the image to a desired form. The question then arises, given the distorted image obtained from such a sensor, if it is possible to unwarp it in software to obtain a true perspective (or some other) view. The answer is that perspective views are attainable if and only if the sensor realizes a central projection, i.e., the set of rays that enter the camera is a bundle over a point. This point is called the virtual viewpoint, and the rays that enter the system may or may not actually pass through the virtual viewpoint, hence its name. A classic example of such a system is the hyperbolic mirror viewed with a camera whose center of projection lies at one focus of the mirror. The other focus then serves as a virtual viewpoint. Such a system was used by Rees⁴ to create a panoramic viewing and projection system. This device made use of an elliptical screen on which the image was projected. Robotics has been an important application area for catadioptric sensors, and an early application to vision-based robotics using a conical mirror was carried out by Yagi and Kawato.⁵ An imaging system with a hyperbolic mirror in which images could be digitally unwrapped was proposed by Yamazawa *et al.*⁶ A system consisting of a parabolic mirror and a narrow-field (orthographic) camera has been studied by Bruckstein and Richardson^{7,8} and by Nayar.⁹

Lenses containing two or more mirrors are considerably more complicated. There are many such systems that are essentially telescope designs.¹⁰ Mirror lenses are available for photographic purposes, such as the above-mentioned Maksukov–Cassegrain. In the case of these narrow-field photographic lenses though, the use of mirrors inherently creates the problem of obstruction. This results in less light-gathering ability, and peculiar, aesthetically unappealing “*bokeh*,” i.e., strange-looking, out-of-focus regions. Some photo-

R. A. Hicks (ahicks@math.drexel.edu) is with the Department of Mathematics, Drexel University, Philadelphia, Pennsylvania 19104. M. Millstone (millstone@cims.nyu.edu) is with the Courant Institute of Mathematical Sciences, New York University, New York, New York 10012. K. Daniilidiis (kostas@grasp.cis.upenn.edu) is with the Department of Computer and Information Science, General Robotics, Automation, Sensing, and Perception (GRASP) Laboratory, University of Pennsylvania, Philadelphia, Pennsylvania 19104.

Received 14 April 2006; revised 17 May 2006; accepted 18 May 2006; posted 24 May 2006 (Doc. ID 69986).

0003-6935/06/287205-06\$15.00/0

© 2006 Optical Society of America

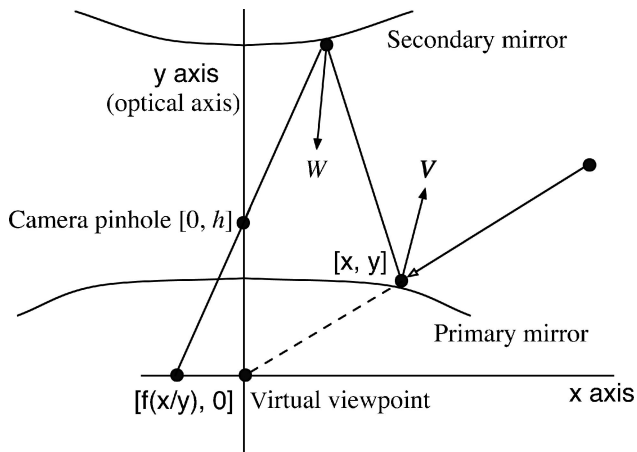


Fig. 1. Seeking two mirrors such that the point $[a, b]$ projects through $[h, 0]$ to $[f(a/b), 0]$.

graphic mirror lenses, such as the Makowsky Kadatron LDM-1 avoid this problem by placing the mirrors off axis. Here we should clarify that the important distinction between these systems and the systems discussed in this paper is that mirror lenses such as the LDM-1 are used for image formation (and have a very narrow field) while the mirror systems we are considering are modeled as being viewed with a pinhole camera model (although for practical purposes, imaging systems similar to those discussed here are constructed by using a conventional camera and lens pointed at a mirror).

An early wide-angle two-mirror system appears in the 1947 patent of Young,¹¹ whose invention is a two-mirror system for panoramic imaging. The camera is placed behind a convex mirror that faces a second mirror. (Presumably, both mirrors were spherical.) Young points out that an advantage of using two mirrors is that it reduces aberrations. A recent analysis of two-mirror systems consisting of conic mirrors was performed by Nayar and Peri.¹² Bruckstein and Richardson^{7,8} also considered two-mirror systems consisting of parabolas and argued that this is the most efficient means of achieving the projection obtained from the combination of a hyperbolic mirror and pinhole camera combination.

The prescribed projection problem for catadioptric sensors is the problem of designing a sensor that realizes a given projection.¹³ In the single mirror, the rotationally symmetric case, any central projection can be obtained in an approximate sense. That is, a sensor can be created that realizes a given projection approximately for distant objects, and the approximation gets better as the objects become more distant. In the single-mirror case though, the only central devices possible must contain a single conic. The main result of this paper is that, in the two-mirror case, any central projection may be achieved exactly by a two-mirror rotationally symmetric system. We describe how this can be achieved and give three examples in Sections 2 and 3.

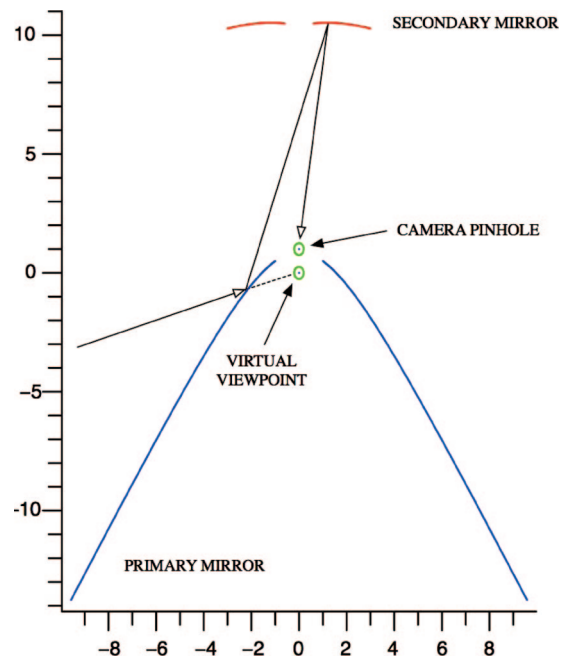


Fig. 2. (Color online) Cross section of a two-mirror system that achieves stereographic projection.

2. Model of the Problem

Suppose we take a 2D coordinate system with $[0, 0]$ as the proposed virtual viewpoint, as in Fig. 1, and the y axis as the optical axis, which is also the axis of symmetry of the system. We describe a pair of mirrors that will image a point $[x, y]$ to a prescribed point $[f(x/y), 0]$, i.e., f is the given projection. We will assume only that the rays reflect according to the angle of incidence being equal to the angle of reflection and that a pinhole camera will form the image. There is no need to introduce any particular system of units, but in all our examples we take the distance h between the virtual viewpoint and the pinhole of the camera to be 1.

We refer to the first mirror that the rays are incident upon as the primary mirror, and the other as the secondary mirror. If we assume that the primary mirror passes through the point $[x, y]$, then the system must image all the points on the line containing $[0, 0]$ and $[x, y]$ to the point $[f(x/y), 0]$. Therefore the point on the secondary mirror corresponding to $[x, y]$ must lie on the line connecting $[f(x/y), 0]$ and the center of projection (pinhole) of the camera at $[0, h]$. As we will see, any point on this line is a viable candidate. Suppose that we parameterize the line at $t \rightarrow [t, -th/f(x/y) + h]$. Then for each choice of x, y , and t , we have a pair of points on the two mirrors $[x, y]$ on the primary and $[t, -th/f(x/y) + h]$ on the secondary.

Each such pair of points determines a pair of normals \mathbf{V} and \mathbf{W} to the primary and secondary mirrors, respectively, at $[x, y]$ and $[t, -th/f(x/y) + h]$. These may be easily calculated. For example, to compute \mathbf{V} , we calculate the unit vector representing the direction from $[x, y]$ to $[t, -th/f(x/y) + h]$ and add it to the

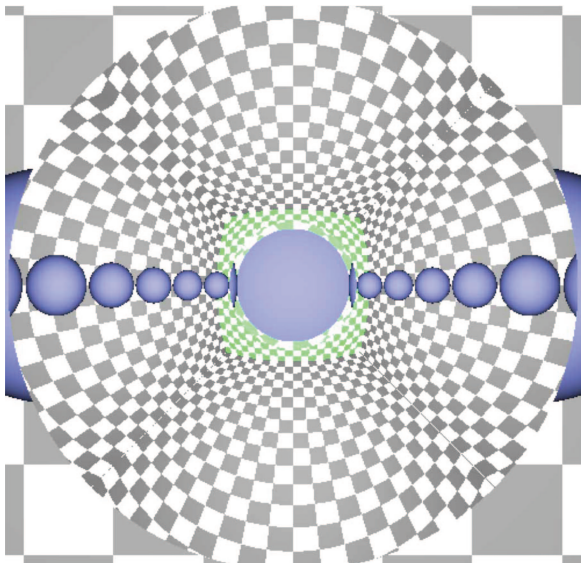


Fig. 3. (Color online) A ray-tracing simulation of an image formed by the system depicted in Fig. 2.

unit vector in the direction of $[x, y]$. These two vectors are not independent of each other—one needs both points in the plane to compute either one of them. To be more precise, one needs $[x, y]$ and t . If we consider the primary curve to be parameterized by $t \rightarrow [x(t), y(t)]$, then the two functions $x(t)$ and $y(t)$ determine the secondary mirror entirely. Taking

$$z(t) = -\frac{th}{f\sqrt{\frac{x(t)}{y(t)}} + h}, \quad (1)$$

we must then have

$$\mathbf{V} = \frac{[x(t), y(t)]}{\sqrt{x(t)^2 + y(t)^2}} + \frac{[t - x(t), z(t) - y(t)]}{\sqrt{[t - x(t)]^2 + [z(t) - y(t)]^2}}. \quad (2)$$

A similar calculation holds for \mathbf{W} . Since \mathbf{W} and \mathbf{V} are constructed to be normal to the curves, their dot product with the tangents to $[x(t), y(t)]$ and $[t, z(t)]$ must be zero, i.e., we have the pair of differential equations

$$[x'(t), y'(t)] \cdot \mathbf{V} = 0, \quad (3)$$

$$[1, z'(t)] \cdot \mathbf{W} = 0. \quad (4)$$

The reader should keep in mind that $z(t)$ is determined by $x(t)$ and $y(t)$. In practice this system is quite complicated, and numerical methods are required to produce solutions. (We give an example of one of the equations written out explicitly below.) Since this system is implicitly given, i.e., it is not of the form

$$x'(t) = F(x(t), y(t), t), \quad y'(t) = G(x(t), y(t), t), \quad (5)$$

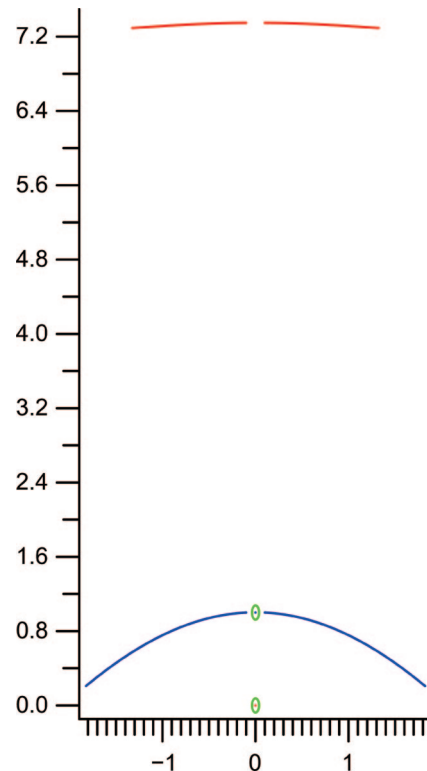


Fig. 4. (Color online) Cross section of a sensor that has equiresolution and is central.

it is not easy to apply the standard existence theorems of differential equations to conclude that solutions to the system exist, or whether numerical approximations will converge to the solutions. Our position on this is that the goal is to find mirror designs. Here we do not focus on these more theoretical issues but rather point to the simulations as

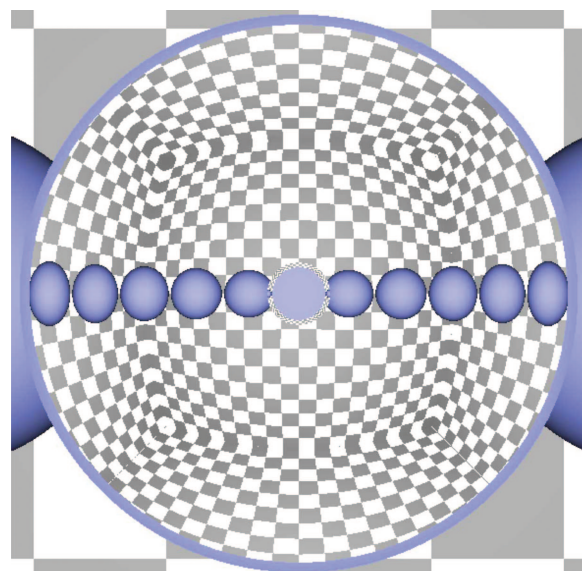


Fig. 5. (Color online) Ray-tracing simulation of an image formed by the system depicted in Fig. 4.

evidence that our model is at least correct in these cases.

3. Three Designs

For all of the examples given below there are numerous choices that had to be made. One must first choose the projection. Even if f is the desired projection, it may be simpler to implement $-f$. Also, one may choose to multiply f by a scalar. The effect of scaling by a small number is to increase the initial height of the secondary mirror. This is important because generally one wants to minimize the amount by which the secondary mirror blocks the primary. Also, initial conditions x_0 , y_0 , and t_0 must be chosen. Note that an initial height for the secondary mirror is not chosen but is $-t_0 h / f(x_0 / y_0) + h$. Finally, one has the choice of solving the differential equations backward or forward. All these choices are important from a design standpoint. For example, presumably one would want

Our first example is a sensor that realizes the stereographic projection, which is given by

$$[x, y] \rightarrow \frac{\alpha x}{\sqrt{x^2 + y^2} - y}. \quad (6)$$

In this example we take $h = 1$, $\alpha = 0.2$, and $t_0 = 3$, $x(t_0) = 0.5$, $y(t_0) = 0.5$, and we solved the differential equations backward in time. The reader should recall that the virtual viewpoint is always $[0, 0]$. In practice, there is a bit of an art to choosing these values, since one must avoid problems such as obstruction, or an awkward distance or ratio of sizes between the mirrors.

Despite the compact form of Eqs. (3) and (4), they have considerable symbolic complexity, which is evident only when they are written in detail. For example, in this case, when written explicitly, Eq. (4) becomes

$$\begin{aligned} & -t - \frac{x(t)}{5\sqrt{x(t)^2 + y(t)^2} - y(t)} \\ & \sqrt{\left(-t - \frac{x(t)}{5\sqrt{x(t)^2 + y(t)^2} - y(t)}\right)^2 + \left(-1 - \frac{[\sqrt{x(t)^2 + y(t)^2} - y(t)]5t}{x(t)}\right)^2} \\ & + \frac{-t + x(t)}{\sqrt{(-t + x(t))^2 + \left(-5\frac{\{\sqrt{x(t)^2 + y(t)^2} - y(t)\}t}{x(t)} + y(t) - 1\right)^2}} \\ & + \left[5\frac{\sqrt{x(t)^2 + y(t)^2} - y(t)}{x(t)} - 5\frac{t(\sqrt{x(t)^2 + y(t)^2} - y(t))}{x(t)^2} \frac{dx}{dt} + 5t\left(\frac{x(t)}{\sqrt{x(t)^2 + y(t)^2}} \frac{dx}{dt} + y(t) \frac{dy}{dt} - \frac{dy}{dt}\right) \right] \\ & \times \left[5\frac{\sqrt{x(t)^2 + y(t)^2} - y(t)}{x(t)} - \frac{5t(\sqrt{x(t)^2 + y(t)^2} - y(t))}{x(t)^2} \frac{dx}{dt} + \frac{5t}{x(t)}\left(\frac{x(t)}{\sqrt{x(t)^2 + y(t)^2}} \frac{dx}{dt} + y(t) \frac{dy}{dt} - \frac{dy}{dt}\right) \right] \\ & \times \left[\frac{\left(-1 - \frac{5t[\sqrt{x(t)^2 + y(t)^2} - y(t)]}{x(t)}\right)}{\sqrt{\left(-t - \frac{x(t)}{5\sqrt{x(t)^2 + y(t)^2} - 5y(t)}\right)^2 + \left(-1 - \frac{5t[\sqrt{x(t)^2 + y(t)^2} - y(t)]}{x(t)}\right)^2}} \right. \\ & \left. + \frac{\frac{-5t(\sqrt{x(t)^2 + y(t)^2} - y(t))}{x(t)} + y(t) - 1}{\sqrt{(-t + x(t))^2 + \left(\frac{-5t(\sqrt{x(t)^2 + y(t)^2} - y(t))}{x(t)} + y(t) - 1\right)^2}} \right] = 0. \end{aligned}$$

the camera of real system embedded inside or behind the primary mirror (as it is in similar existing designs), and so the position of the camera pinhole relative to the primary mirror is important. Another design factor that is historically important is that using multiple mirrors makes for a more compact system.

As with the other two examples below, Eqs. (3) and (4) were solved numerically and the data points exported to a ray tracer. Figure 2 depicts the cross section of the system. Figure 3 is a ray-tracing simulation of the system using a cubical test room with gray and white checkerboard walls, and a ring of spheres centered in the room about the sensor, with

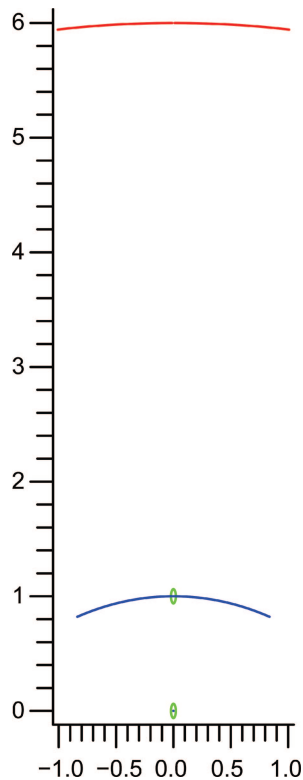


Fig. 6. (Color online) Cross section of a sensor that achieves a wide-angle perspective projection.

the centers of each pair of adjacent spheres differing by 30° .

The theorem of Geyer and Daniilidis¹⁴ states that the projection induced by the coupling of a parabolic mirror and an orthographic projection can be factored into a map to the sphere (normalization) followed by stereographic projection. A consequence of this factorization is the fact that such sensors send lines and circles to lines and circles. This property may be exploited in the calibration from images of lines and in the computation of epipolar geometry of an image pair.^{15,16} In our example, the correctness of our design is verified by the fact that the spheres appear to be circular in the image.

As mentioned in the previous paragraph, there is a single mirror sensor that realizes this projection by using an orthographic camera. However, a single-mirror central system does not exist that is based on a perspective camera model and realizes stereographic projection. (Note that it is not the case that a hyperbolic mirror coupled with a perspective projection results in stereographic projection.)

Next, we consider equiresolution systems. On the one hand, central single-mirror systems must contain mirrors that have conic cross sections. On the other, Hicks and Perline¹⁷ classified the mirrors that give rise to equiresolution projections, i.e., any two equal solid angles are afforded the same number of pixels in the image. Since these systems are rotationally symmetric, there is only one projection

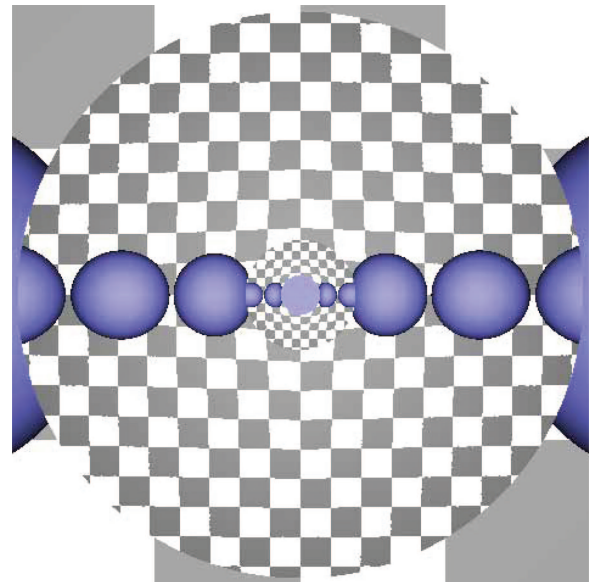


Fig. 7. (Color online) Ray-tracing simulation of an image formed by the system depicted in Fig. 6.

with this property:

$$[x, y] \rightarrow \alpha \sqrt{2(1 - \cos[\pi/2 - \arctan(y/x)])}. \quad (7)$$

The single-mirror systems described in Ref. 17 are not central, and the above projection is valid only for infinitely far points. Nevertheless, by using two mirrors as described above, this corresponding projection can be realized as a central two-mirror system. In this case we took $h = 1$ and $\alpha = 0.16$ and $t_0 = 0.1$, $x(t_0) = 0.1$, $y(t_0) = 1$ and solved the equations forward in time. See Figs. 4 and 5 for the resulting pair and simulation. In this case the correctness of our design is verified by the fact that the spheres all appear to have the same area in the image.

Finally we consider a rectifying pair of mirrors, i.e., a pair that gives a wide-angle perspective view. In this case we took $h = 1$ and $\alpha = -0.2$ and $t_0 = 0.01$, $x(t_0) = 0.01$, $y(t_0) = 1$ and solved the equations forward in time. Figures 6 and 7 depict the result. Here the crucial parameter is the field of view, which is simply controlled by the scale factor in the projection

$$[x, y] \rightarrow \alpha \frac{x}{y}. \quad (8)$$

The correctness of our design is verified by the fact that the checkerboard appears undistorted.

4. Summary and Conclusions

In computer vision, the aberration of distortion is a topic of great interest. On the one hand, the goal may be to remove it via software transformations, and on the other it may be exploited for applications such as camera calibration. We have given differential equations that allow one to design central systems to re-

alize any central projection. This is done directly by solving the equations, rather than by using a traditional optimization commonly found in optical design. Using this method we have demonstrated three unusual imaging devices but have addressed only the aberration of distortion, and essentially assumed that a real camera with an appropriate dioptric component could be found to create images that are in focus, which has been the traditional approach in the design of catadioptric sensors in computer vision. Clearly it would be ideal to have an approach in which the minimization of aberrations was incorporated into the differential equations.

The authors acknowledge the support provided by the following National Science Foundation grants: NSF-IIS-0083209, NSF-IIS-0121293, NSF-EIA-0324977, NSF-CNS-0423891, NSF-IIS-0431070, NSF-DMS-0211283, and NSF-IIS-0413012, as well as the Army Research Office, Multidisciplinary Research Initiative ARO/MURI DAAD19-02-1-0383.

References

1. R. Kingslake, *A History of the Photographic Lens* (Academic, 1989).
2. L. H. Kleinschmidt, "Apparatus for producing topographic views" U.S. patent 994,935 (13 June 1911).
3. R. A. Hicks, "The page of catadioptric sensor design," <http://www.cs.drexel.edu/ahicks/design/design.html> (2003).
4. D. Rees, "Hyperbolic ellipsoidal real time display panoramic viewing installation for vehicles," U.S. patent 3,229,576 (18 January 1966).
5. Y. Yagi and S. Kawato, "Panoramic scene analysis with conic projection," in *Proceedings of the International Conference on Robots and Systems* (IEEE, 1990), pp. 1–10.
6. K. Yamazawa, Y. Yagi, and M. Yachida, "Omnidirectional imaging with hyperboidal projection," in *Proceedings of the IEEE International Conference on Robots and Systems*, (IEEE, 1993), pp 77–86.
7. A. Bruckstein and T. Richardson, *Omniview Cameras with Curved Surface Mirrors* (Bell Laboratories Technical Memo, 1996).
8. A. Bruckstein and T. Richardson, "Method and system for panoramic viewing with curved surface mirrors," U.S. patent 5,920,376 (6 July 1999).
9. S. Nayar, "Catadioptric omnidirectional camera," in *Proc. Computer Vision Pattern Recognition* (IEEE Computer Society Press, 1997), pp. 482–488.
10. M. Bass, ed. *Handbook of Optics* (McGraw-Hill, 1995), Vol. II.
11. W. A. Young, "Wide-angle optical system," U.S. patent 2,430,595 (11 November 1947).
12. S. Nayar and V. Peri, "Folded catadioptric cameras," in *Proc. Computer Vision Pattern Recognition* (1999), pp. 217–223.
13. R. A. Hicks, "Designing a mirror to realize a given projection." *J. Optical Soc. Am. A* **22**, 323–330 (2005).
14. C. Geyer and K. Daniilidis, "Catadioptric camera calibration," in *Proceedings of the Seventh International Conference on Computer Vision* (1999), pp. 398–404.
15. C. Geyer and K. Daniilidis, "Mirrors in motion: Epipolar geometry and motion estimation," in *Proceedings of the Eleventh International Conference on Computer Vision* (2003), pp. 766–773.
16. C. Geyer and K. Daniilidis, "Para-cata-dioptic calibration," *IEEE Trans. Pattern Anal. Mach. Intell.*, **24**, 687–694 (2002).
17. R. Hicks and R. Perline, "Equireolution catadioptric sensors," *Appl. Opt.* **44**, 6108–6114 (2005).